

MEASUREMENTS OF TRANSVERSE BEAM DIFFUSION RATES IN THE FERMILAB TEVATRON COLLIDER*

G. Stancari[†], G. Annala, T. R. Johnson, D. A. Still, A. Valishev
Fermi National Accelerator Laboratory, Batavia, IL 60150, USA

Abstract

The transverse beam diffusion rate vs. particle oscillation amplitude was measured in the Tevatron using collimator scans. All collimator jaws except one were retracted. As the jaw of interest was moved in small steps, the local shower rates were recorded as a function of time. By using a diffusion model, the time evolution of losses could be related to the diffusion rate at the collimator position. Preliminary results of these measurements are presented.

Phenomena related to stochastic transverse beam dynamics in circular accelerators can be described in terms of particle diffusion [1, 2, 3, 4, 5]. It was demonstrated that these effects can be observed with collimator scans [6] (Figure 1). For the Tevatron, a detailed description of the collimation system can be found in Ref. [7]. Collimator jaws define the machine aperture. If they are moved towards the beam center in small steps, typical spikes in the local shower rate are observed, which approach a new steady-state level with a characteristic relaxation time (Figure 2). When collimators are retracted, on the other hand, a dip in losses is observed, which also tends to a new equilibrium level. These phenomena were used to estimate the diffusion rate in the beam halo in the SPS at CERN [8], in HERA at DESY [6], and in RHIC at BNL [9]. Similar measurements were carried out at the Tevatron in 2011 to characterize the beam dynamics of colliding beams and to study the effects of the novel hollow electron beam collimator [10].

A diffusion model of the time evolution of loss rates caused by a step in collimator position was used to interpret the data [11]. It builds upon the work presented in Ref. [6] and its main assumptions: constant diffusion rate within the range of the step and linear halo tails. These two hypotheses allow one to obtain analytical expressions for the solutions of the diffusion equation and for the corresponding loss rates as a function of time. Our extended model addresses some of the limitations of the previous model and generalizes it in the following ways: (a) losses before, during, and after the step are predicted; (b) different steady-state rates before and after are explained; (c) determination of the model parameters (diffusion coefficient, tail population, detector calibration, and background rate) is more robust and precise.

Following Ref. [6], we consider the evolution in time t of a beam of particles with phase-space density $f(J, t)$ described by the diffusion equation

$$\partial_t f = \partial_J (D \partial_J f),$$

where J is the Hamiltonian action and D the diffusion coefficient. The particle flux at a given location $J = J'$ is $\phi = -D \cdot [\partial_J f]_{J=J'}$. During a collimator step, the action $J_c = x_c^2 / \beta_c$, corresponding to the collimator position x_c at a ring location where the amplitude function is β_c , changes from its initial value J_{ci} to its final value J_{cf} during a time Δt . The step in action is $\Delta J \equiv J_{cf} - J_{ci}$. In the Tevatron, typical steps are $50 \mu\text{m}$ in 0.2 s , and the amplitude

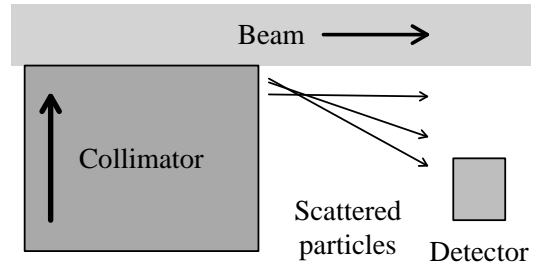


Figure 1: Schematic diagram of the apparatus.

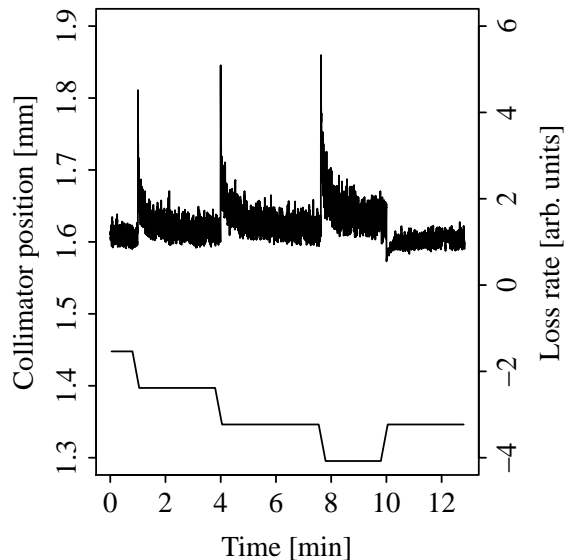


Figure 2: Example of the response of local loss rates to inward and outward collimator steps.

* Fermi Research Alliance, LLC operates Fermilab under Contract No. DE-AC02-07CH11359 with the US Department of Energy. This work was partially supported by the US LHC Accelerator Research Program (LARP).

[†] On leave from Istituto Nazionale di Fisica Nucleare, Sezione di Ferrara, Italy. E-mail: stancari@fnal.gov.

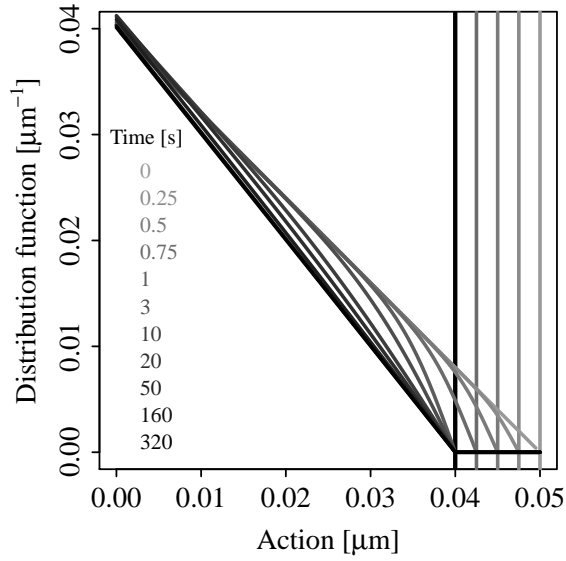


Figure 3: Calculated evolution of the distribution function during an inward collimator step. The vertical lines represent the positions of the collimator vs. time. Collimator action varies between $J_{ci} = 0.05 \mu\text{m}$ and $J_{cf} = 0.04 \mu\text{m}$ in a time $\Delta t = 1 \text{ s}$. The initial and final slopes of the tails are $A_i = 0.8 \mu\text{m}^{-2}$ and $A_f = 1 \mu\text{m}^{-2}$. The diffusion coefficient is $D = 10^{-5} \mu\text{m}^2/\text{s}$.

function is tens of meters. It is assumed that the collimator steps are small enough so that the diffusion coefficient can be treated as a constant in that region. This hypothesis is justified by the fact that the fractional change in action is of the order of $\Delta J_c/J_c \sim (2)(25 \mu\text{m})/(2 \text{ mm}) = 2.5\%$. Because the diffusion coefficient is a strong function of action ($D \sim J^4$), this translates into a variation of 10% in the diffusion rate, an acceptable systematic in a quantity that varies by orders of magnitude. If D is constant, the diffusion equation becomes $\partial_t f = D \partial_{JJ} f$. With these definitions, the particle loss rate at the collimator is equal to the flux at that location: $L = -D \cdot [\partial_J f]_{J=J_c}$. Particle showers caused by the loss of beam are measured with scintillator counters placed close to the collimator jaw. The observed shower rate is parameterized as $S = kL + B$, where k is a normalization constant including detector acceptance and efficiency and B is a background term which includes, for instance, the effect of residual activation. Both k and B are assumed to be independent of collimator position and time during the scan.

Under the hypotheses described above, the diffusion equation can be solved analytically using the method of Green's functions, subject to the boundary condition of vanishing density at the collimator and beyond. Details are given in Ref. [11]. An example of the evolution of the phase-space density according to this model is shown in Figure 3. A few representative snapshots in time are chosen: during collimator movement ($0 \leq t \leq \Delta t$); a short time after the step, with a time scale determined by

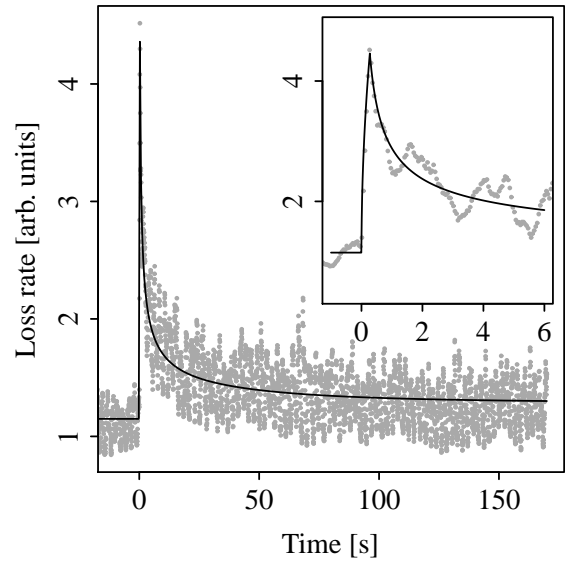


Figure 4: Example of least-squares fit of the model to the observed loss rates during an inward collimator step.

$|J_{ci} - J_{cf}|^2/D = 10 \text{ s}$; and a long time after the step, with a characteristic time $J_c^2/D = 160 \text{ s}$.

Local losses are proportional to the gradient of the distribution function at the collimator. The gradients differ in the two cases of inward and outward step, denoted by the I and O subscripts, respectively:

$$\begin{aligned} \partial_J f_I(J_c, t) &= -A_i + 2(A_i - A_c)P\left(\frac{-J_c}{\sigma}\right) + \frac{1}{\sqrt{2\pi}\sigma} \cdot \\ &\cdot \left\{ -2A_i(J_{ci} - J_c) + 2(A_i J_{ci} - A_c J_c) \exp\left[-\frac{1}{2}\left(\frac{J_c}{\sigma}\right)^2\right] \right\} \\ \partial_J f_O(J_c, t) &= -2A_i P\left(\frac{J_{ci} - J_c}{\sigma}\right) + 2(A_i - A_c)P\left(\frac{-J_c}{\sigma}\right) + \\ &+ 2\frac{A_i J_{ci} - A_c J_c}{\sqrt{2\pi}\sigma} \exp\left[-\frac{1}{2}\left(\frac{J_c}{\sigma}\right)^2\right]. \end{aligned}$$

The parameters A_i and A_f are the slopes of the distribution function before and after the step, whereas A_c varies linearly between A_i and A_f as the collimator moves. The parameter σ is defined as $\sigma \equiv \sqrt{2Dt}$; its effect is to expose the dependence of losses on the inverse square root of time, as is typical for diffusion processes. The function $P(x)$ is the S-shaped cumulative Gaussian distribution function: $P(-\infty) = 0$, $P(0) = 1/2$, and $P(\infty) = 1$.

The above expressions are used to model the measured shower rates. Parameters are estimated from a least-squares fit to the experimental data. An example is shown in Figure 4, where the best-fit function from the model is superimposed on the data points. The inset shows a detail of the first few seconds after the collimator step. The oscillations in the data are due to coherent beam jitter. The background B is measured before and after the scan when the

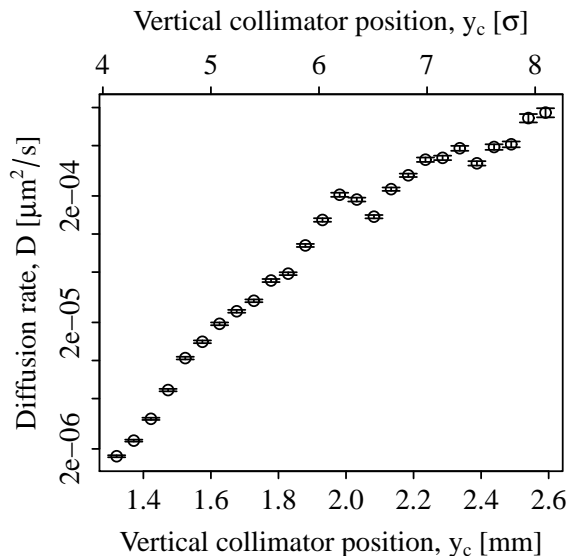


Figure 5: Measurements of the transverse beam diffusion rate with a vertical antiproton collimator scan (Tevatron Store 8527, 25 February 2011).

jaws are retracted. The calibration of kA_i and kA_f is estimated by comparing the level of losses with beam intensity and lifetime. In practice, D is determined by both the measured relaxation time and by the value of the peak (or dip) in losses.

The model explains the data very well when the diffusion time is long compared to the duration of the step. With this technique, the diffusion rate can be measured over a wide range of amplitudes. At large amplitudes, the method is limited by the vanishing beam population and by the fast diffusion times. The limit at small amplitudes is given by the level of tolerable loss spikes.

Several collimator scans were performed at the Tevatron during 2011. The goal was to observe the effect on diffusion of beam-beam forces and of the hollow electron beam scraper. An example of the strong dependence of the diffusion rate on amplitude between $4\sigma_y$ and $8\sigma_y$ is shown in Figure 5. (Here σ_y is the root-mean-square vertical beam size.) The experiment was done at the end of a regular collider store. Experimental conditions are summarized in Table 1. Every 2 to 3 minutes, the F48 vertical antiproton collimator was moved inward by $50 \mu\text{m}$. At the location of the collimator the amplitude function was $\beta_y = 29 \text{ m}$ and the r.m.s. beam size was $\sigma_y = 320 \mu\text{m}$.

In this experiment, the diffusion rate grows with the 9th power of amplitude, or $J^{4.5}$. It exhibits some structure, possibly related to the nonlinearities of the machine. Only random uncertainties are shown in Figure 5. Because the Tevatron collimator jaws are one-sided, the main systematic error, which is estimated not to exceed 30%, comes from the absolute position of the collimator with respect to the beam axis. A detailed comparison of the diffusion rates for antiprotons with and without collisions will be presented in a separate report. For the bunches affected by the hollow

Table 1: Summary of experimental conditions for the diffusion measurement shown in Figure 5: instantaneous luminosity, \mathcal{L} ; average number of protons and antiprotons per bunch, N^p and N^a ; average transverse emittances (95%, normalized), ϵ_x^p , ϵ_y^p , ϵ_x^a , and ϵ_y^a ; average longitudinal emittances, ϵ_z^p and ϵ_z^a ; average momentum spreads, δ_p and δ_a ; average incoherent tunes, Q_x^p , Q_y^p , Q_x^a , and Q_y^a ; chromaticities, Q'_x and Q'_y .

\mathcal{L}	N^p	N^a	ϵ_x^p	ϵ_y^p	ϵ_x^a	ϵ_y^a
$1/(\mu\text{b s})$	10^{11}	10^{11}	μm	μm	μm	μm
27	1.67	0.326	38.0	42.7	26.2	21.7

ϵ_z^p	ϵ_z^a	δ_p	δ_a
eVs	eVs	10^{-4}	10^{-4}
7.18	6.97	1.753	1.708

Q_x^p	Q_y^p	Q_x^a	Q_y^a	Q'_x	Q'_y
0.5888	0.5888	0.5861	0.5862	4.0	4.4

beam scraper, this technique provided the first direct evidence of halo diffusion enhancement (about a factor 10).

The authors would like to thank H. J. Kim and T. Sen (Fermilab) for discussions and insights. These measurements would not have been possible without the support of the Fermilab Accelerator Division personnel. In particular, we would like to thank M. Convery, C. Gattuso, and R. Moore.

REFERENCES

- [1] A. J. Lichtenberg and M. A. Leiberman, *Regular and Chaotic Dynamics* (Springer-Verlag, New York, 1992), p. 320.
- [2] T. Chen et al., Phys. Rev. Lett. **68**, 33 (1992).
- [3] A. Gerasimov, FERMILAB-PUB-92-185 (1992).
- [4] F. Zimmermann, Part. Accel. **49**, 67 (1995); SLAC-PUB-6634 (1994).
- [5] T. Sen and J. A. Ellison, Phys. Rev. Lett. **77**, 1051 (1996).
- [6] K.-H. Mess and M. Seidel, Nucl. Instrum. Methods Phys. Res. A **351**, 279 (1994); M. Seidel, Ph.D. Thesis, Hamburg University, DESY-94-103 (1994).
- [7] M. Church et al., in Proc. 1999 Part. Accel. Conf. (PAC99), p. 56; N. Mokhov et al., to be published in JINST (September 2011), FERMILAB-PUB-11-378-APC.
- [8] L. Burnod, G. Ferioli, and J. B. Jeanneret, CERN-SL-90-01 (1990).
- [9] R. P. Fliiller III et al., in Proc. 2003 Part. Accel. Conf. (PAC03), p. 2904.
- [10] G. Stancari et al., Phys. Rev. Lett. **107**, 084802 (2011); arXiv:1105.3256 [phys.acc-ph]; these proceedings, WEOAD02.
- [11] G. Stancari, arXiv:1108.5010 [physics.acc-ph], FERMILAB-FN-0926-APC (2011).